CHAOTIC OSCILLATIONS IN DYNAMIC POSITIONING OF TELEOPERATED UNDERWATER VEHICLES SUBJECT TO WAVE AND CURRENT PERTURBATIONS

Mario Alberto Jordán* and Jorge Luis Bustamante

Argentinean Institute of Oceanography (IADO-CONICET),
Dep. of Electrical Engineering and Computers (DIEC),
Universidad Nacional del Sur (UNS),
Florida 8000, CRIBABB, B8000FWB Bahía Blanca,
ARGENTINA

Abstract: This paper is concerned with the study of nonlinear oscillations in servotracking control systems for the teleoperation of ROVs subject to strong currents and harmonic waves. Particularly, the case of variable cable length during tactics on the sea bottom such as sea bottom scanning and systematic grab sampling are analyzed. The route to chaos from predictable period-one oscillations is studied using the cable length magnitude and rate, the current intensity, and wave amplitude and frequency as main bifurcation parameters.

Keywords: Nonlinear oscillations, Control of oscillations, Time-varying cable/body system, Nonlinear control system, Remotely operated vehicles.

1. INTRODUCTION

The appearance of nonlinear oscillations in moored floating structures has been pointed out by many authors (see for instance Ellerman *et al.*, 2002; Jordán and Beltrán, 2004). They frequently appear when a structure is forced to oscillate by action of waves and strong flows.

Tethered vehicles (TVs) like tow fishes and remotely operated underwater vehicles (ROVs) are two special cases of moored systems with much more motion freedom for tracking purposes than semisubmersible moored structures. While the first class is represented by towed bodies, the second one possesses self propulsion to navigate in 6 degrees of freedom. Nevertheless both ship-cable-vehicle systems show similar behaviors when perturbations on the cable due to current and surface waves dominate significantly the dynamics (Prabhakar and Buckham, 2005, Jordán and Bustamante, 2006).

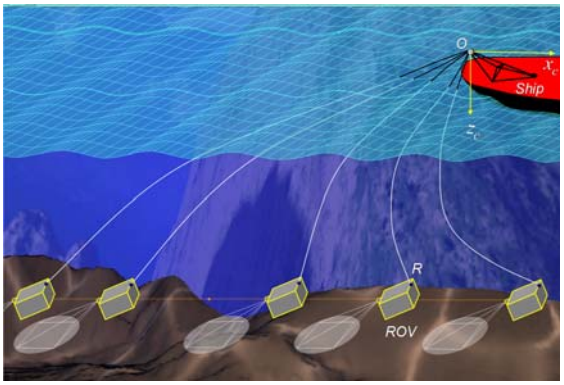

Figure 1 - Sea bottom scanning with servocontrolled ROV

Apart from their passive and active motions in TVs and ROVs, respectively, between both classes there exists other fundamental difference, which

* Corresponding author: Mario A. Jordán. E-mail: mjordan@criba.edu.ar. Tel. +54-291 4861309, Ext. 169, Fax: +54-291 486-1527/1112/1519.

is related to the variable cable length in ROVs in contrast with the almost always fixed length of the towing line in TVs. A variable cable length facilitates particular tactics in their operations, as for instance, to scan in the water column or irregular ocean bottom for grab sampling (Jordán and Bustamante, 2007).

From a physical point of view, the cable shape and the position of the attach points play a decisive roll in the vehicle oscillatory behavior when harmonic waves are present. From a mathematical point of view, particular motions of the cable-vehicle system are described by a Mathieu equation parametrized in a set of bifurcation parameters like cable length, stiffness, wave amplitude and frequency, and current intensity. One important particularity of the dynamics is the so-called "taut-slack" phenomenon which makes motion to be chaotic or unpredictable for tracking or positioning (Jordán and Bustamante, 2004). Also there was found a solid evidence of a wide diversity in oscillatory behaviors in one dimension, including period doubling and chaos (Jordán and Bustamante, 2006b).
The modelling of the cable effects in the dynamics of ROVs for 6 degrees of freedom under strong flow currents was published in (Jordán *et al.*, 2006). Similarly, the study was extended to waves acting on the pivot point of the umbilical cable on the mother ship (Jordán and Bustamante, 2006a).

In this present paper a study of nonlinear oscillations are undertaken for ROVs deployed in estuarial missions under strong currents involving a variable cable length. The end here is to provide a theoretical analysis of this system in 3D in the context of a servotracking problem for ROVs under this operation conditions.

2. QUASI-STATIONARY MODEL OF THE CABLE

A possible configuration of the ship-cable-ROV system is illustrated in Fig. 1, where a submersed ROV hangs from a crane on a mother ship. Herein, a perturbation originated by the ocean stream causes the ROV to be dragged in the x-z plane in favor of the flow. This produces moments which instabilize its desired course. Also a wave action can eventually induce cable tugs from the support point.
Here, it is assumed that the cable remains entirely confined in a plane defined by the directrix $\overline{AA}$ containing the point O on the crane tackle and the point R on the attach extreme of ROV (see Fig.2). Also the plane can eventually hinge about the directrix $\overline{AA}$ when the ROV moves sideways. The hinge angle α is determined by the ROV-coordinates taken with respect to O. One notices also that the upper section of the cable $\overline{OO'}$ is over the water line, while the section $\overline{O'R}$ is completely submersed.
The flow is considered stationary and laminar with intensity variation only in the depth. Additionally, the cable is assumed to have neutral buoyancy. The ROV coordinates in the x-y-z frame at O being $[l_{ROV}, h\sin\alpha, h\cos\alpha]^T$.

2.1 Orbit of the support point

Consider a fixed point $\bar{O}$ and a frame of references with center on it. Suppose now the ship is anchored and that a harmonic wave excitation on the ship produces an elliptic motion of O about $\bar{O}$ in the vertical plane as illustrated in the figure. So, the orbit of O about $\bar{O}$ is

$$\begin{cases} x_O(t) = a_x \cos\omega t \\ z_O(t) = a_y \sin\omega t \end{cases} . \tag{1}$$

where a_x and a_y are the ellipse radii.
On the other side, the coordinates of R are (*cf.* Fig. 2)

$$x_R(t) = l_{ROV}(t) - a_x \cos(\omega\ t) \tag{2}$$

$$z_R(t) = \frac{(h_{ROV}(t) + a_y \sin(\omega\ t))}{\cos\alpha(t)} \tag{3}$$

$$\alpha(t) = \tan^{-1}\left(\frac{h_{ROV}(t) + a_y \sin(\omega\ t)}{s_{ROV}(t)}\right). \tag{4}$$

and the projection of coordinates in the hinged plane onto the vertical plane yields

$$x(t) = x_c(t) + a_x \cos(\omega t) \tag{5}$$

$$z(t) = -z_c(t)\cos\alpha(t) + a_y \sin(\omega t). \tag{6}$$

The coordinates of O' on the hinged plane are obtained with help of (5)-(6) as

$$b_1 = \frac{b + a_y \sin(\omega t)}{\cos\alpha(t)}, \tag{7}$$

where b is the coordinate z of O' on the vertical plane and $\alpha = \tan^{-1}(s_{ROV}/h_{ROV})$. Clearly, O' also lies on the cable plane.

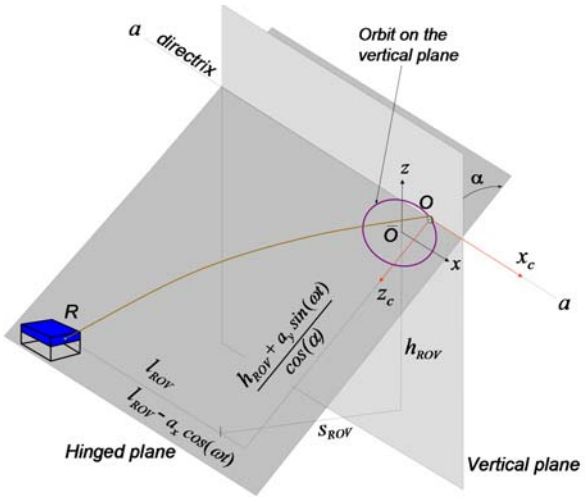

Figure 2 - Elliptic motion of the winch pivot

2.2 Equations

The force relations on the cable satisfy (see Fig. 3)

$$T\frac{dx_c}{dp} + H - \int_{b_1}^{z_c} \frac{\partial f_D}{\partial \bar{z}_c} d\bar{z}_c = 0 \tag{8}$$

$$T\frac{dz_c}{dp} + W\frac{s}{L_a} = V \tag{9}$$

$$\left(\frac{dx_c}{dp}\right)^2 + \left(\frac{dz_c}{dp}\right)^2 = 1 \tag{10}$$

$$T = EA_0\left(\frac{dp}{ds} - 1\right), \tag{11}$$

where s is the so-called unstretched Lagrangian coordinate and analogously p the stretched Lagrangian coordinate of the profile with $dp = \sqrt{dx_c^2 + dz_c^2}$; $s = L_a$ at point O', L_a is the unstretched cable length on $\overline{OO'}$ with a weight W, $\frac{\partial f_D}{\partial z_c}(z_c)$ is the load distribution function of the drag force in the direction z_c; T is the cable tension at s; and V and H are modulus of the vertical and horizontal reactive forces at extreme O, respectively. Now, let us consider the sections $\overline{OO'}$ of length L_a and $\overline{O'R}$ of length L_w separately.

2.3 General solution of cable profile

The solution of (8)-(10) will be different according to the stretch, namely on air or in water. As a general solution is however very involved, we tackle better the solution by sections instead.

2.3.1. Cable on air To this end, let us first to deal with the upper portion $\overline{OO'}$. Accordingly, with $\frac{\partial f_D}{\partial z_c} = 0$ and from (8)-(11) one achieves (*cf.* Jordán and Beltrán, 2004)

$$T(s) = \sqrt{H^2 + \left(V - W\frac{s}{L_a}\right)^2} \tag{12}$$

$$x_c(s) = \frac{Hs}{EA_0} + \frac{HL_b}{W}\left(\sinh^{-1}\frac{V}{H} - \sinh^{-1}\frac{V - \frac{Ws}{L_a}}{H}\right) \tag{13}$$

$$z_c(s) = \frac{WL_a}{EA_0}\left(\frac{V}{W} - \frac{s}{2L_b}\right) + \frac{HL_b}{W}\left(\sqrt{1+\left(\frac{V}{H}\right)^2} - \sqrt{1+\left(\frac{V - W\, s/L_a}{H}\right)^2}\right). \tag{14}$$

The weight W corresponding to the cable of length L_a is

$$W = g\rho_w \frac{\pi D^2}{4} L_a. \tag{15}$$

with D the diameter and $\rho = \rho_w$ the water density. The coordinates of the crossing point O' are calculated from (13) and (14) as $a_1 = x_c(L_a)$ and $b_1 = z_c(L_a)$, respectively. The length L_a will be calculated later.

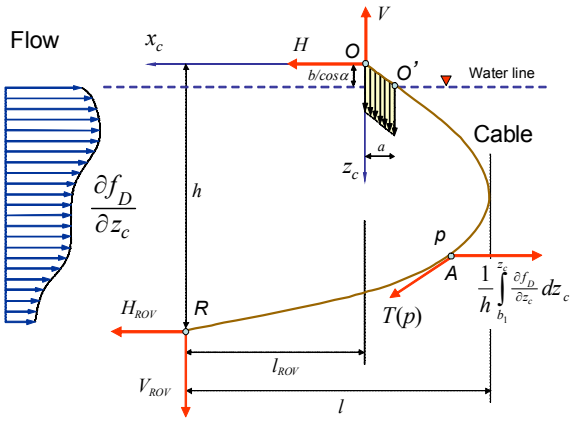

Figure 3 - Foces in the cable plane x_c-z_c

2.3.2. Cable in sea water On the other hand, for the section $\overline{O'R}$ the weight disappears while the drag force takes its place as a distributed load. The flow rate is referred to as u_c and assumed from now on constant in the depth. Thus, one can apply the Morison's law and one attains (Fig. 3)

$$F_D(z_c) = \int_{b_1}^{z_c} \frac{\partial f_D}{\partial \bar{z}_c} d\bar{z}_c = \int_{b_1}^{z_c} \frac{\rho_w\, D\, C_d\, u_c^2}{2}\, d\bar{z}_c \tag{16}$$

$$= \frac{\rho_w\, D\, C_d\, u_c^2}{2}(z_c - b_1), \tag{17}$$

with C_D the drag coefficient for slender cylinders. Combining (8)-(9) for $s > L_a$, it is valid

$$\frac{dx_c}{dz_c} = \frac{\int_{b_1}^{z_c} \frac{\partial f_D}{\partial \bar{z}_c} d\bar{z}_c - H}{V - W}. \tag{18}$$

Then, integrating (18) it results for $z_c \geq b_1$

$$x_c(z_c) = x_c(L_a) + \frac{1}{V\text{-}W}\int_{b_1}^{z_c}\left(\int_{b_1}^{\check{z}_c} \frac{\partial f_D}{\partial \bar{z}_c} d\bar{z}_c \text{-} H\right) d\check{z}_c. \tag{19}$$

Unlike to the cable shape in the air with a catenary form, the shape of the cable submersed assumes a quadratic form for constant rate profiles. Certainly, one attains

$$x_c(z_c) = x_c(L_a) - \frac{H}{V\text{-}W}(z_c\text{-}b_1) + \frac{\rho_w\, D\, C_d\, u_c^2}{4\,(V\text{-}W)}(z_c\text{-}b_1)^2, \tag{20}$$

with $x_c(L_a)$ obtained from (13).

2.4 Forces

The tension of the cable is obtained by combining (8)-(10). It is valid for $0 \leq s \leq L_a$ (cable section on air)

$$T(s) = \sqrt{H^2 + \left(V - g\rho_w \frac{\pi D^2}{4} s\right)^2}, \tag{21}$$

and for $z_c \geq b_1$. For the point R the forces are

$$H_{ROV} = F_D(h) - H, \quad V_{ROV} = \left(V - \frac{g\rho_w\, \pi D^2 L_a}{4}\right). \tag{22}$$

The forces H and V of point O will be determined later.

2.5 Moments

For the particular case (16) acting on the vertical segment $\overline{O'R}$, The moment with respect to R is

$$h\ H + l_{ROV}\ V - \frac{\rho_w\ D\ C_d\ u_c^2}{2}\frac{(h-b_1)^2}{2} - \\ - \left(l_{ROV} + \frac{a_1}{2}\right)\frac{g\rho_w\ \pi D^2 L_a}{4} = 0. \quad (23)$$

with

$$a_1 = \frac{HL_b}{EA_0} + \frac{4H}{g\pi D^2 \rho_w}\left(\sinh^{-1}\frac{V}{H} - \sinh^{-1}\frac{V - \frac{g\pi D^2 L_a \rho_w}{4}}{H}\right). \quad (24)$$

2.6 Cable length

The study of elastic interactions of the ship-cable-ROV system involves strengths in both lengths, *i.e.*, in p and s. Here, they are referred to as the stretched and unstretched lengths

$$\bar{L} = \int_0^L \frac{dp}{ds} ds \quad (25)$$

$$L = \int_0^L ds, \quad (26)$$

respectively. The unstretched length L can be measured at the revolving spool of the ship crane system exactly, while the stretched length $\bar{L}$ has to be calculated from model with positions and forces on the cable ends O and R.

Accordingly, one can calculate from (14) with $s = L_a$ and $EA_0 >> \frac{W}{H}\left(V - \frac{W}{2}\right)$

$$L_a = \frac{V - H\sqrt{\left(\sqrt{1+\left(\frac{V}{H}\right)^2} - \frac{g\rho_w \frac{\pi D^2}{4}}{H}\frac{b + a_y \sin(\omega t)}{\cos\alpha(t)}\right)^2 - 1}}{g\rho_w \frac{\pi D^2}{4}}, \quad (27)$$

where (7) and (15) were employed therein.

On the other hand, the length of the section $\overline{O'R}$ for the submersed cable is achieved indirectly by calculating first the cable length L. To this end, let us determine first $\frac{ds}{dz_c} = \frac{dp}{dz_c}\frac{ds}{dp}$ from (9) and (11) for $s \geq L_a$ and positions h and b_1. So, after integration, it is valid

$$L - L_a = \int_{L_a}^{L} ds = \int_{b_1}^{h} \frac{ds}{dz_c} dz_c = \quad (28)$$

$$= \int_{b_1}^{h} \frac{T}{V - g\rho_w \frac{\pi D^2}{4}} \frac{EA_0}{EA_0 + T} dz_c =$$

$$= EA_0 \int_{b_1}^{h} \frac{\sqrt{\left(\frac{H - \frac{\rho_w D C_d u_c^2 (z_c - b_1)}{2}}{V - g\rho_w \frac{\pi D^2}{4}}\right)^2 + 1}}{EA_0 + \frac{\sqrt{\left(\frac{H - \frac{\rho_w D C_d\ u_c^2 (z_c - b_1)}{2}}{V - g\rho_w \frac{\pi D^2}{4}}\right)^2 + 1}}{1/\left(V - g\rho_w \frac{\pi D^2}{4}\right)}} dz_c.$$

The last integral has been solved by symbolic programming with MATHEMATICA® 5.0. Due to space restriction this large result is not transcribed here. Generically, this yields

$$L = L_a + G(u_c, b_1, h, H, V), \quad (29)$$

where G is a multivariable expression to be evaluated numerically in our next study.

3. DETERMINATION OF UPPER CABLE FORCES

The determination of H and V is not straightforward because many equations involve variables explicitly, *i.e.*, there exist no close expressions for solving the problem of forces and cable profile analytically. So, we aim to an exact but numerical solution.

Toward this goal, following algorithm is proposed in (Jordán *et al.*, 2006; Pinna-Cortiñas *et al.*, 2006), and redefined here for elastic cords. A close solution is developed for uniformly distributed drag loads. This consists in:

1. Start-up. Use starting values for b, l_{ROV}, h, L, D, EA_0, a_y, ρ_w and C_d. Also a constant flow rate u_c is provided.
2. Calculate $F_D(h)$ according to (17)
3. Solve the nonlinear equations (29) with (27) and (23) with (24) for V and H recursively, *e.g.*, by employing a gradient-base searching algorithm. For starting the iterations use $V_0 = \frac{\rho_w\ D\ C_d\ u_c^2 (h-b_1)}{4}\tan\left(\sin^{-1}\left(\frac{h-b_1}{L}\right)\right)$ and $H_0 = \frac{\rho_w\ D\ C_d\ u_c^2 (h-b_1)}{4}$ as initial conditions.
4. Calculate the force components H_{ROV} and V_{ROV} on the ROV by means of (22)
5. Calculate the cable form (13)-(14) for $z_c \leq b_1$ and (19) for $b_1 < z_c \leq h$.

   Our experience shows that the convergence of step 3 is reached after a few iterations (in average less than 20 with "*fzero*" of MATLAB® 7.0 (R14)).

4. APPLICATION TO ROV CONTROL

One of the main elements in the ship-cable-ROV system is the control exerted on the ROV in its flight path or regulation about one fixed point. It is usually based on a model of the vehicle. In this section, we will describe a high-performance control system for ROVs in 6 degrees of freedom. Details are given in (Jordán and Bustamante, 2006c).

Consider the ROV dynamics given by

$$M\dot{\mathbf{v}}_r = -C(\mathbf{v}_r)\mathbf{v}_r - D(|\mathbf{v}_r|)\mathbf{v}_r + \mathbf{F}_b(\boldsymbol{\eta}) + \mathbf{F}_c + \mathbf{F}_t \quad (30)$$

$$\dot{\boldsymbol{\eta}} = J(\boldsymbol{\eta})\mathbf{v}_r, \quad (31)$$

with the matrices

$$M = M_b + M_a \quad (32)$$

$$C(\mathbf{v}_r) = C_b. \times C_0(\mathbf{v}_r) + C_a. \times C_0(\mathbf{v}_r) \quad (33)$$

$$D(|\mathbf{v}_r|) = D_l + D_q\,\mathrm{diag}(|\mathbf{v}_r|), \quad (34)$$

where the generalized position in the earth-fixed frame is denoted by $\boldsymbol{\eta} = [x, y, z, \phi, \theta, \psi]^T$, $\mathbf{v}_r = [u_r, v_r, w_r, p_r, q_r, r_r]^T$ indicates the generalized relative velocity vector in its flight path in a body-fixed frame, $J(\boldsymbol{\eta})$ is a well-known rotation matrix depending on the Euler angles ϕ and θ, M is the inertia matrix composed by the body

inertia matrix M_b and the added mass matrix M_a that accounts for the surrounded fluid mass, C is the centripetal and Coriolis matrix with a first component $C_b.\times C_0$ for the body dynamics and a second component $C_a.\times C_0$ for the hydrodynamics, the operation ".×" denotes element-by-element multiplication of constant matrices C_b and C_a times a state-dependent matrix C_0, D is the damping matrix composed by a constant matrix and a velocity-depending matrix, $\mathbf{F}_b$ is the net buoyancy force, $\mathbf{F}_c$ the cable reaction force, and $\mathbf{F}_t$ the generalized thrust (see Jordán and Bustamante, 2006c). Moreover, C_b, C_a, D_l, and D_q are constant matrices and the notations $\text{diag}(\mathbf{v}_r)$ and $\text{diag}(|\mathbf{v}_r|)$ mean $\text{diag}(u_r,...,r_r)$ and $\text{diag}(|u_r|,...,|r_r|)$, respectively.

The cable force on the ROV depends on fixed-earth coordinates. In order to project it onto the main axis of the moving vehicle we state first

$$\mathbf{F}'_c = J_1^{-1}\left[-H_{ROV}, -V_{ROV}\sin\alpha, V_{ROV}\cos\alpha\right]^T, \quad (35)$$

where J_1 is the upper block matrix of J and $\mathbf{F}'_c$ is the force on the point R in the vehicle-fixed axis. Finally, the cable force is a generalized force with the form

$$\mathbf{F}_c = \left[\mathbf{F}'_{c_x}, \mathbf{F}'_{c_y}, \mathbf{F}'_{c_z}, -c_z\mathbf{F}'_{c_x}, c_z\mathbf{F}'_{c_x}+c_x\mathbf{F}'_{c_z}, -c_x\mathbf{F}'_{c_x}\right]^T, \quad (36)$$

where the c_x and c_z are the coordinates x and z, respectively, of R with respect to G.

We employ a fixed controller that determines the generalized thrust by feeding back the states $\boldsymbol{\eta}$ and $\mathbf{v}_r$. So, it is valid

$$\mathbf{F}_t = C(\mathbf{v}_r)\mathbf{v}_r + D_l\mathbf{v}_r + D_q\,\text{diag}(|\mathbf{v}_r|)|\mathbf{v}_r + \quad (37)$$
$$+\mathbf{F}_b(\boldsymbol{\eta}) + M\mathbf{d}\left(\boldsymbol{\eta}, \overset{\curvearrowleft}{\boldsymbol{\eta}}, \overset{\curvearrowleft}{\mathbf{v}}_r, t\right) - K_v\overset{\curvearrowleft}{\mathbf{v}}_r - J^T(\boldsymbol{\eta})\overset{\curvearrowleft}{\boldsymbol{\eta}} - \mathbf{F}_c,$$

with

$$\mathbf{d}(\overset{\curvearrowleft}{\boldsymbol{\eta}}, \overset{\curvearrowleft}{\mathbf{v}}_r, \boldsymbol{\eta}, t) = \frac{d}{dt}\left(J^{-1}(\boldsymbol{\eta})\left(\boldsymbol{\eta}_{ref} - \dot{\boldsymbol{\eta}}_c\right)\right) - \frac{dJ^{-1}}{dt}K_p\overset{\curvearrowleft}{\boldsymbol{\eta}} +$$
$$+ J^{-1}(\boldsymbol{\eta})K_p^2\overset{\curvearrowleft}{\boldsymbol{\eta}} + J^{-1}u_c - J^{-1}(\boldsymbol{\eta})K_pJ(\boldsymbol{\eta})\overset{\curvearrowleft}{\mathbf{v}}_r, \quad (38)$$

and $\overset{\curvearrowleft}{\boldsymbol{\eta}}$ and $\overset{\curvearrowleft}{\mathbf{v}}_r$ being positioning and cinematic errors in a tracking navigation problem defined as

$$\overset{\curvearrowleft}{\boldsymbol{\eta}} = \boldsymbol{\eta} - \boldsymbol{\eta}_{ref} \quad (39)$$

$$\overset{\curvearrowleft}{\mathbf{v}} = \mathbf{v}_r - J^{-1}(\boldsymbol{\eta})\left(\dot{\boldsymbol{\eta}}_{ref} - \dot{\boldsymbol{\eta}}_c\right) + J^{-1}K_p\overset{\curvearrowleft}{\boldsymbol{\eta}}, \quad (40)$$

where $\dot{\boldsymbol{\eta}}_c$ is the flow velocity vector in the earth-fixed frame, which has u_c as the unique element.

Therefore, the control action (37) entails the perturbation of the cable force $\mathbf{F}_c$ in (36), which is supposed here known for the study and unknown for the controller in (37).

5. SIMULATION

We carry out experiments to illustrate the features of the proposed control of nonlinear oscillations. They are fitted to the setup of to Table I according to the Fig. 1 which was taken as case study.

Table I. Setup parameters for experiments

Param.	Value	Param.	Value
C_D	0.9	$(l_{ROV})_{ref}$	variable (m)
L	$[20 \div 60](m)$	$(h)_{ref}$	$20(m)$
$\dot{L}$	$[.05 \div .061](\frac{m}{s})$	u_c	$-0.15(\frac{m}{s})$
ρ_w	$1021(Kg/m^3)$	b	$0(m)$
D	$2\times10^{-2}(m)$	a_x	$0.5(m)$
EA_0	$\infty(N)$	a_y	$0.35(m)$
ω	$1.5(Hz)$	u	$[0. \div 0.1](\frac{m}{s})$

Figs. 4-5-6 describe a mission concerning the regulation of the ROV about $(x,z) = (45.65, 20)(m)$, in where the cable length is extended from $L = 50(m)$ to $60(m)$ at a rate $\dot{L} = 0.05(m/s)$. As the figures clearly show, the transition of L involves the route to chaos from a period-one oscillation. The evolution of the cable force is becoming softer when the cable is lengthened.

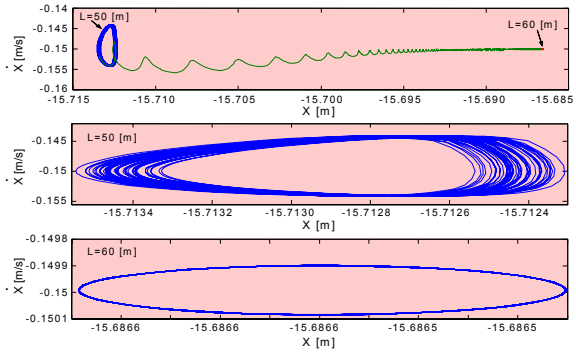

Figure 4 - Phase portrait for mode x. Transition from $L = 50(m)$ to $60(m)$ (top), regulation with $L = 50(m)$ (middle) and $L = 60(m)$ (bottom).

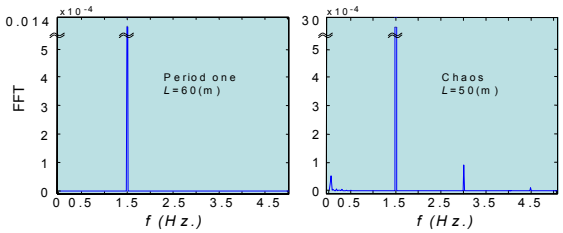

Figure 5 - FFT of mode x. Period one for $L = 50(m)$ (left) and chaos for $L = 60(m)$ (right).

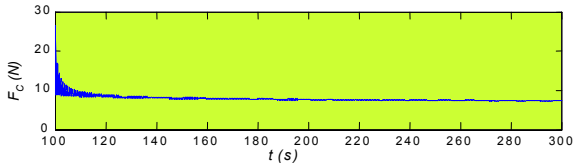

Figure 6 - Cable force in the transition from $L = 50(m)$ to $L = 60(m)$

The second experiment concerns the path-following navigation of the ROV along a stretch at constant depth and rate of displacement. Herein, the cable length transits from $L = 22(m)$ up to $L = 50.5(m)$ at $\dot{L} = 0.061(m/s)$. Figs. 7 and 8 depict the evolution of the advance coordinate x in phase portrait

and the ROV cable force. Clearly, the transitions of qualitative behaviors evolve dynamically. The nonlinear oscillation starts with period one and then increases its power chaotically when tending to $L = 50(m)$. Also the cable force increases with chaotic evolution.

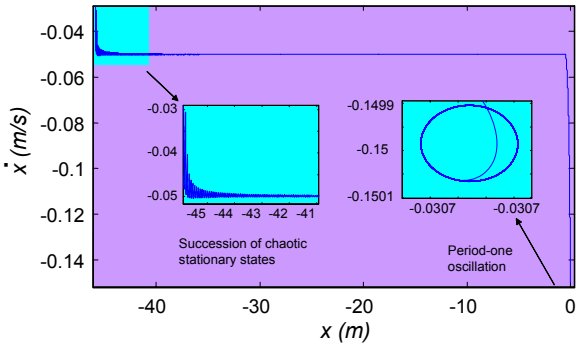

Figure 7 - Phase portrait for the mode x in a path-following control case (L variable)

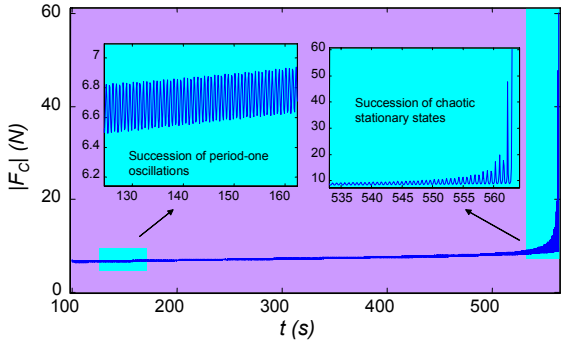

Figure 8 - Cable force evolution in a path-following control case (L variable)

6. CONCLUSIONS

This paper has dealt with the study of controlled nonlinear oscillations in navigation of ROVs subject to strong currents and harmonic waves. Particularly, the case of sampling missions with variable cable length are focused in the investigation. A model for quasi-stationary dynamics of a ship-cable-ROV system was developed together with a high-performance control system for attenuating perturbations similar to cable tugs in form of nonlinear oscillations. The mean position of the ROV is selected as the main bifurcation parameter in the study.

The analysis reveals that nonlinear oscillations are quite possible in ROV navigation and teleoperation. In our study, transits from period-one oscillation to chaos (and vice versa) in both regulation and tracking control cases of the vehicle were clearly evidenced. Therein, it was worth noticing that chaotic scenarios are associated with large increments of the cable force even without causing thrust saturation.

7. ACKNOWLEDGEMENTS

The authors wish to thank IADO-CONICET and DIEC-UNS for the funding of this investigation.

REFERENCES

[1] El-Hawary, F., "The ocean Engineering Handbook," *CRC Press LLC*, 2001.

[2] Ellermann, K., Kreuzer, E., Markiewicz, M.: Nonlinear Dynamics of Floating Cranes. Nonlinear Dynamics **27**(2), ,107-183, 2002.

[3] Fossen, T.I., "Guidance and Control of Ocean Vehicles," *John Wiley&Sons,* UK, 1994.

[4] Jordán, M.A. and Beltrán Aguedo R., "Nonlinear identification of mooring lines in dynamic operation of floating structures," *Ocean Engineering*, **31**, 455-482, 2004.

[5] Jordán, M.A., and Bustamante J.L., "Análisis de Oscilaciones No-Lineales en Sistemas Complejos de Mecánica e Hidrodinámica - Herramientas y Metodología," *Revista Iberoam. de Autom. e Inform. Ind.* (RIAI, ISSN 1697-7912, España), 63-77, 2004.

[6] Jordán M.A. and Bustamante J.L., "Harmonic Perturbation of Umbilical Cable in Adaptive Controlled Underwater Vehicles," *XX^o Cong. Arg. de Control Aut.*, Aug. 28-30, Buenos Aires, Argentina, 2006a.

[7] Jordán, M.A. and Bustamante, J.L., "Numerical Stability Analysis and Control of Umbilical-ROV Systems in Taut-Slack Condition," in press, *Nonlinear Dynamics*, 2006b.

[8] Jordán, M.A., Bustamante, J.L. and Beltrán-Aguedo, R., "An Approach for Modeling the Dynamics of ROV-Cable Control Systems in Tidal-Inlet Environments," in *Int. Conf. of the Fac. of Elec. Eng., FIE06*, Santiago de Cuba, Cuba, July 12-14, 2006.

[9] Jordán M.A. and Bustamante J.L., "A Speed-Gradient Adaptive Control with State/ Disturbance Observer for Autonomous Subaquatic Vehicles," Accepted for *45th. IEEE Conf. on Dec. and Control*, San Diego, CA, USA, Dec. 11-13, 2006c.

[10] Jordán M.A. and Bustamante J.L., "An Adaptive Control System for ROVs in Discrete Sampling Missions with Time-Optimal Characteristics," Submitted to *IEEE American Control Conference ACC07*, Ref. 1528, New York, USA, July 2007.

[11] Mavrakos, S.A., Papazoglou, V.J., Triantafyllou, M.S., Chatjigeorgiou, I.K., "Deep water mooring dynamics," *Marine Structures*, **9**, 181-209, 1996.

[12] Prabhakar S. and Buckham, B., "Dynamics Modeling and Control of a Variable Length Remotely Operated Vehicle Tether," *Proc. of OCEANS05 MTS/IEEE*, 2005.

[13] Pinna-Cortiñas J.M., Jordán, M.J. (Director) and Bustamante, J.L.(Codirector). "Estudio de Perturbaciones en Vehículos Subacuáticos con Cable," Student Diss., Univ. Nac. del Sur, *DIEC-IADO/GCAIO*, 2006.